Article ID: 1000-324X(2019)05-0567-06 **DOI:** 10.15541/jim20180383

Ceramic/Resin Composite Powders with Uniform Resin Layer Synthesized from SiO_2 Spheres for 3D Technology

SUN Zhi-Qiang, YANG Xiao-Bo, WANG Hua-Dong, LI De-Li, LI Shu-Qin, LÜ-Yi

(Aerospace Institute of Advanced Materials & Processing Technology, Beijing 100074, China)

Abstract: Ceramic/resin composite powders used for 3D printing are synthesized by micro-sized SiO_2 dense spheres through a simple method, and their consolidation and sintering performances are fully characterized. The results show that the viscosity of coating media decreases gradually with the increasing temperature or decreasing the resin content and the most suitable resin content is 27wt%. The uniformly coated ceramic/resin composite spheres with well dispersity, fine fluidity (25 (s/50 g)) and larger packing density (45.0%) are successfully synthesized. The spherical shape of ceramic powders is revealed to be the vital factor for the achievement of uniform coating layers, because of the interconnected packed pores and the uniform cohesive energy of spheres. Meanwhile, the thickness (1.1−3.7 μm) of coating layer is controlled precisely through changing the pressure during the filtration process. Moreover, the synthesized powders show well consolidation performance for the favorite necks among spheres. After sintered at 1250 ℃, the ceramics with compressive strength of 10.2 MPa and bending strength of 2.7 MPa are obtained while the shrinkage is only 5%, which indicates the composite spheres have an advantage in improving the precision of 3D technology.

Key words: powder technology; SiO_2 spheres; 3D printing; coating layer

Owing to the freedom in design and flexibility, additive manufacturing (AM) offers new opportunities for shaping techniques of ceramics[1-2], especially in aerospace industry (*eg.* silica wave-transmitting material). Indirect selective laser sintering (SLS) is one of the AM technologies for ceramic production, which based on ceramic/resin composite powders and its selective curing by means of lasers[3-4]. This technology avoids the difficulty of ceramic sintering by lasers, and the ceramic greens can be achieved at lower temperature by melting organic binders. The content of binders is usually below 10wt% and it will be removed sufficiently in the later sintering, which has no harmful effect on the ceramic products. At present, this technology has become a research hotspot and attracted a great attention.

The binders can be added in various methods, and surface coating is an effective way to satisfy indirect SLS[5], which can achieve more homogeneous mixture of ceramic powders and resin. The binders are usually alcohol-soluble (or water-soluble) phenolic resin, which can realize physical coating based on wettability between alcohol (or water) and ceramic particles.

The characteristics of employed powder are the vital factors for SLS technology. The powders with well dispersity, fine fluidity, larger packing density and well sintering controllability will facilitate the 3D printing technology[6]. At present, irregular ceramic powders are commonly used for indirect SLS, although they have poor dispersity and fluidity for the existence of large amount of agglomerated particles. Moreover, the relative packing density of ceramic greens from irregular powders is only about 30%~35% and larger shrinkage (>25%) of ceramics is inevitable in later sintering[7-8]. Besides, uneven shrinkage is unavoidable for the ceramics synthesized by irregular powders, which results in structural defects and degrade the mechanical properties of ceramics[9]. However few studies focus on the morphology of ceramic particles in indirect SLS technology.

As we known, spherical ceramic particles have regular shape and they cannot form agglomerates easily[10], hence they have better dispersity and fluidity. Meanwhile, ceramic spheres are beneficial to fill the larger interstices among spheres, which results in the larger packing density[11]. Moreover, ceramic spheres can avoid uneven shrinkage during later sintering[12], which favors the uniform microstructure of ceramics[13] and facilitates the strengthening of its mechanical performances. Besides, the surface energy of spherical powders is evenly distributed which may benefit the achievement of uniformly coating layers. Hence, it is a good strategy to synthesize

Received date: 2018-08-31; **Modified date:** 2018-11-20
Foundation item: National Natural Science Foundation of China (51802298)
Biography: SUN Zhi-Qiang (1989–), male, Master degree, engineer. E-mail: sunzhiqiang1203@126.com

composite powders from ceramic spheres to solve the difficulties for indirect SLS technology.

In this paper, spherical SiO_2 particles (SSPs) with dense body were adopted to produce ceramic/resin spheres. A simple manufacture method was employed to maintain the spherical shape and well dispersity of composite powders. The obtained composite powders were fully characterized, and their consolidation performance and sintering behavior were revealed as well.

1 Experimental

1.1 Materials

SSPs (purity>99%, d_{10}=6.7 μm, d_{50}=17.3 μm, d_{90}=33.5 μm, ShanChu Co., GuangZhou, China) and alcohol-soluble phenolic resin (1901, ShengQuan Co., ShanDong, China) were used to synthesize composite spheres. SSPs were synthesized from irregular SiO_2 particles (purity>99%, d_{10}=7.4 μm, d_{50}=19.7 μm, d_{90}=37.3 μm, ShanChu Co., GuangZhou, China) through spheroidizing process by thermal plasma, and these irregular particles were also employed in our research to verify the superior packing density of ceramic spheres. Ethanol (Beijing Chemical Works, China) was employed as solvent and hexamethylenetetramine (GuangFu Co., TianJin, China) was adopted as curing agent.

1.2 Preparation of the composite powders

The ceramic/resin composite spheres are synthesized through physical process, and the procedures are illustrated in Fig. 1. Firstly, phenolic resin and curing agent (mass ratio 10∶1) were dissolved in a certain amount of ethanol at 60 ℃, and a yellow solution which served as coating media was achieved. Then, SSPs were added into coating media and a slurry with solid content of 50wt% was obtained. Subsequently, the slurry was heated at a higher temperature of 80 ℃ until the volume of slurry decreased to 75%. Crucially, extraction filtration was carried out under negative pressure of 0.1–0.3 MPa, in which process a large amount of resin was removed. Finally, the filter cake was dispersed in water, and the desired composite spheres were obtained after drying at 60 ℃ for 5 h.

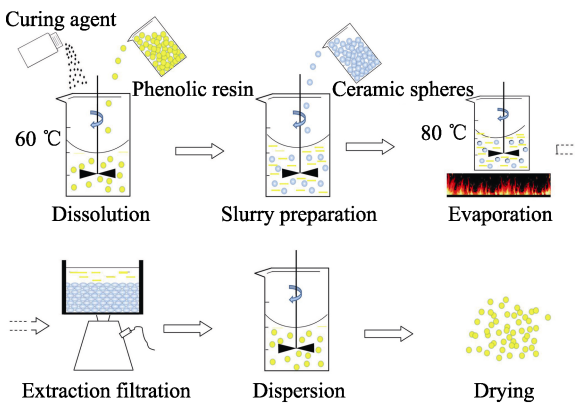

Fig. 1 Schematic of fabrication for ceramic/resin composite powders

1.3 Characterization

The viscosity of coating media was tested by viscometer (NCY, SRD Shanghai). Scanning electron microscope (SEM, JEOL, JSM-6700F) was used to observe the morphology of SiO_2 spheres before and after coating, and their internal structures were observed by Backscatter electron (BSE) detectors. Laser particle size analyzer (Beckman Coulter, LS 13 320) was used to determine the particle size distribution, and the density of spheres ($\rho_{\text{sphere or composite sphere}}$) was measured by pycnometer. The content of coated resin was detected by TG-DSC (NETZSCH STA 449C) at a heating rate of 10 ℃/min.

Hall velocimeter was employed to measure the fluidity (GB 1482-84) and packing density (GB1482-84) of powders. The relative density of packing spheres can be obtained by the following equation:

$$R=\rho_{\text{packing density}}/\rho_{\text{sphere or composite sphere}} \quad (1)$$

The liner shrinkage of sintered ceramics was calculated by dimensional measurements. The compressive strength of consolidated bulk was measured by universal testing machine under a crosshead speed of 0.5 mm/min, and the compressive and bending strength of sintered ceramics were tested at the same conditions.

2 Results and discussion

2.1 Study of coating media

The properties of coating media, including resin content, viscosity and temperature have vital effect on coating process and hence the resin slurry should be studied firstly. The resin slurries with content of 22%, 27% and 32% were prepared respectively, and their viscosities were measured at different temperatures. The results are shown in Fig. 2, as can be seen, the viscosity of slurry decreases gradually with the temperature increasing or the resin content decreasing, and this phenomenon is in coincidence with the common regulation.

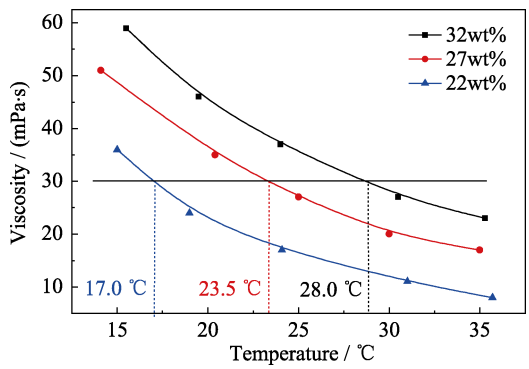

Fig. 2 Effect of temperature and solid content on viscosity of resin slurry

According to the earlier results based on experiments, the coating process can be finely processed when the slurry viscosity is around 30 mPa·s, and the corresponding temperatures of slurries with different resin contents are 17.0, 23.5 and 28.0 ℃ respectively. Obviously, the resin slurry with 27wt% solid content (23.5 ℃, 30 mPa·s) is more suitable to operate at room temperature (20–25 ℃). Consequently, the 27wt% is chosen as the optimized solid content of coating media in this research.

2.2 Characterization of powders before/after coating

Figure 3(a) shows SEM image of employed SSPs. It can be seen that the particles have good sphericity and well dispersity. The density of the spheres is 2.18 g/cm^3, which indicates the spheres are relatively dense and are not composed by loosely packed aggregates. The fluidity and relative packing density of employed SSPs measured by Hall velocimeter is 22 (s/50 g) and 46.2% respectively. It is noted that the irregular powders (the raw material of SSPs) with similar grain size of SSPs are also measured, and the corresponding data is 43 (s/50 g) and 34.5% respectively. By contrast, the advantages of SSPs in fluidity and packing density are obvious, and it can be ascribed to their regular shape and dense body.

The microstructure of the coated particles synthesized at negative pressure of 0.2 MPa is shown in Fig. 3(b), and it can be seen that the shape of powders keeps spherical and the well dispersity is reserved. The uniform coating layer of spheres can be observed clearly from the cross-section image of Fig. 3(c), and the thickness of the coating layer is around 2 μm. The particle size distributions of ceramic spheres and coated spheres are shown in Fig. 3(d), showing that they are similar with each other while the size of the coated ones is slightly larger, which reconfirms the uniformly coated spheres with well dispersity. Unsurprisingly, the d_{50} of synthesized composite spheres is 19.3 μm, which is a little larger than that of the raw spheres (d_{50}=17.3 μm).

Slight degradation on fluidity and relative packing density is found for the synthesized composite spheres (25 (s/50 g) and 45.0%) as compared with SSPs, which may be caused by decrease of particle density (2.10 g/cm^3). Besides, the weight change of the coating layer is only 5.88wt% measured by TG analysis up to 800 ℃.

From above characterization, it can be concluded that uniformly coated ceramic/resin composite spheres with well dispersity, fine fluidity and larger packing density are successfully synthesized by micro-sized SiO_2 dense spheres in this work.

2.3 Mechanism of coating process

The formation procedure of coating layer is also revealed in this work. First of all, the extra resin around packed spheres is removed during extraction filtration. Then, the packed spheres become a filter cake and a liquid

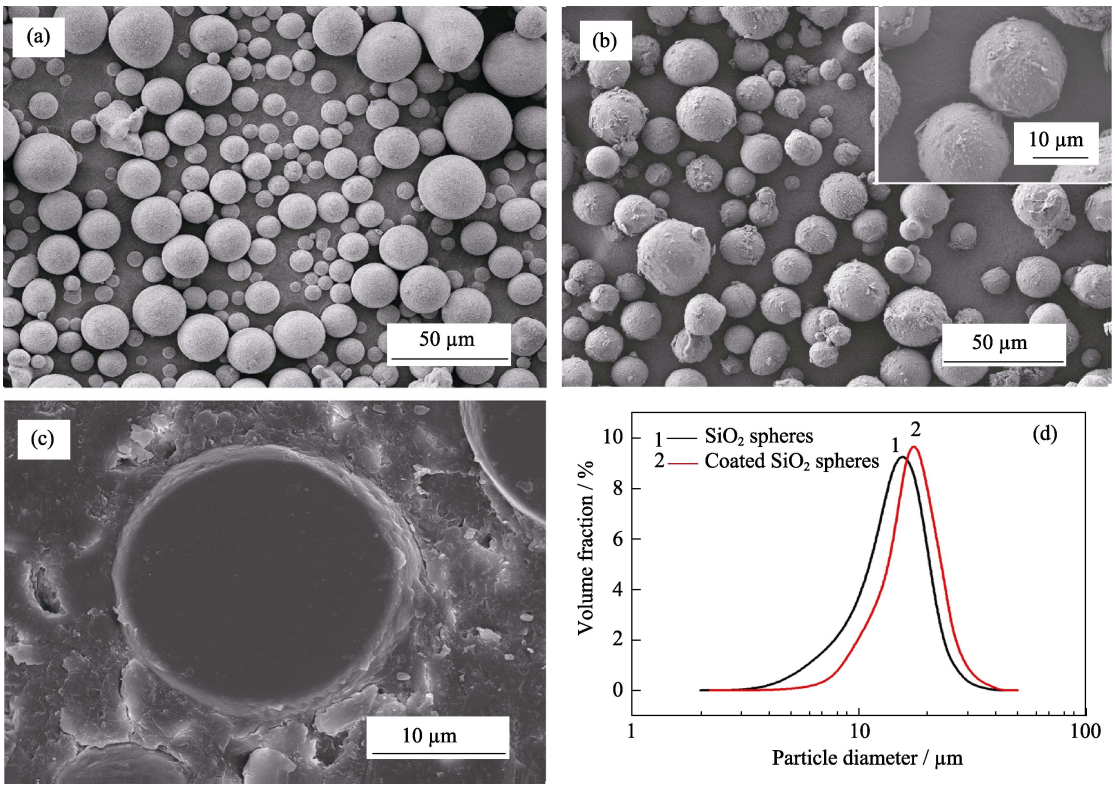

Fig. 3　SEM images of SiO_2 spheres (a), coated spheres (b), the cross section of coating layer (c), and particle size distribution before/after coating (d)

layer composed by ethanol and dissolved resin forms at the surface of spheres with the help of interfacial energy[14]. At last, spheres are dispersed in water and the resin layer is *in-situ* precipitated because of the little solubility of resin in water (20 ℃).

The vital factor for the successful achievement of uniform coating layer is the spherical shape of ceramic powders. On one hand, the pores among packed ceramic spheres are interconnected, and no dead pores exist. The extra resin can be passed out sufficiently, which brings in the formation of liquid layers on spheres. On the other hand, the uniform layer thickness is also related to the spherical shape. As we know, coating process depends on the surface energy, which is also referred to cohesive energy in solid-liquid interphase[15]. Cohesive energy strongly depends on sphere size or curvature[15], while that is definite for a certain sphere. Hence, the sphere surface has uniform cohesive force to keep the soluble resin and uniform coating layer is finally synthesized.

2.4 Control of coating thickness

The coating thickness is controlled through changing the negative pressure in filtration process, and the SEM images of obtained composite spheres are shown in Fig. 4. As can be seen, the composite powders processed at vacuum pressure of 0.1–0.3 MPa are all spherical, and a higher negative pressure results in a thicker coating layer (1.1–3.7 μm). Unsurprisingly, the corresponding content of resin increases from 1.78wt% to 8.41wt% along with the increased layer thickness.

In filtration process, resin is pulled out of packing pores with the help of negative pressure, while cohesive force in solid-liquid interphase resists this process. A lower vacuum pressure provides a greater force to fight the cohesive strength[16], and more resin is removed with a thinner coating layer remaining.

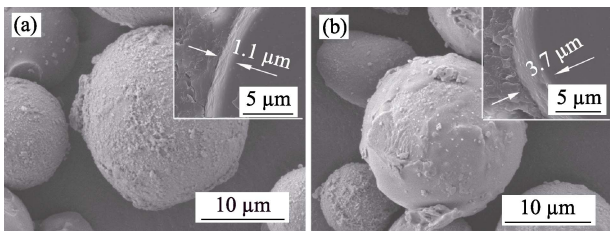

Fig. 4 SEM images of composite spheres and corresponding coating layer fabricated at different negative pressures
(a) 0.1 MPa; (b) 0.3 MPa

2.5 Consolidation performance

The powders fabricated at negative pressure of 0.2 MPa are shown in Fig. 5(a). As can be seen, it is yellow in color which is the same color as the employed resin. After heated at 180 ℃ for only 2 min, the loosely stacked composite spheres were consolidated into a bulk (Fig. 5(b)) without visible shrinkage. The compressive strength of the consolidated bulk is 0.8 MPa, which is strong enough for later polish (Fig. 5(c)). By contrast, the compressive strength of consolidated bulk composed by irregular composite particles is tested to be only 0.3 MPa, which may be caused by the smaller packing density (34.5%). The contrast experiment provides direct evidence of better consolidation performance of spheres. To further explore the variation of the packed powders in the heat-treatment, the fracture surface of obtained bulk is characterized, as can be seen in Fig. 6, the resin necks (red circle) among spheres are formed obviously, and it is certain that the ceramic strength comes from these powerful necks. It's worth noting that sphere surface in consolidated bulk becomes smooth, and it provides some evidences on the formation process of favorite necks: the resin layer is melted at 180 ℃, and then the capillary force arising from the surface tension among neighboring particles provides a driving force for the movement of melt[17]. Unsurprisingly, the necks are finally obtained at the contact points of spheres.

2.6 Sintering performance

Fig. 7 shows the characterization of SiO_2 ceramics synthesized by the composite spheres with layer thickness of 2 μm after consolidated and sintered at 1250 ℃ for 2 h. Fig. 7(a) is the SEM image of the fracture surface of ceramic, exhibiting that the uniformly arranged particles are sintered together and the sintered necks among spheres can be easily observed. The pores are mostly composed of the cell walls of spheres and no blockages derived from uneven shrinkage can be found. The narrow pore size distribution shown in Fig. 7(b) also indicates the ceramics are well structured without structural defects.

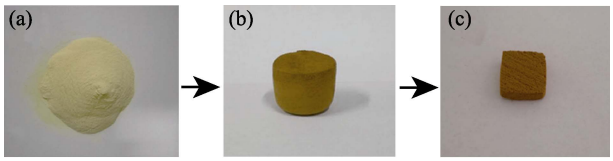

Fig. 5 Photographs of (a) composite powders, (b) consolidated bulk and (c) polished bulk

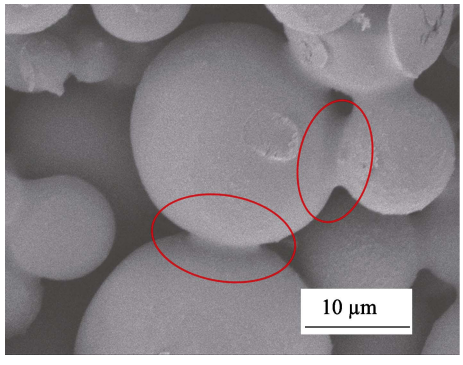

Fig. 6 SEM image of microstructure of consolidated bulk

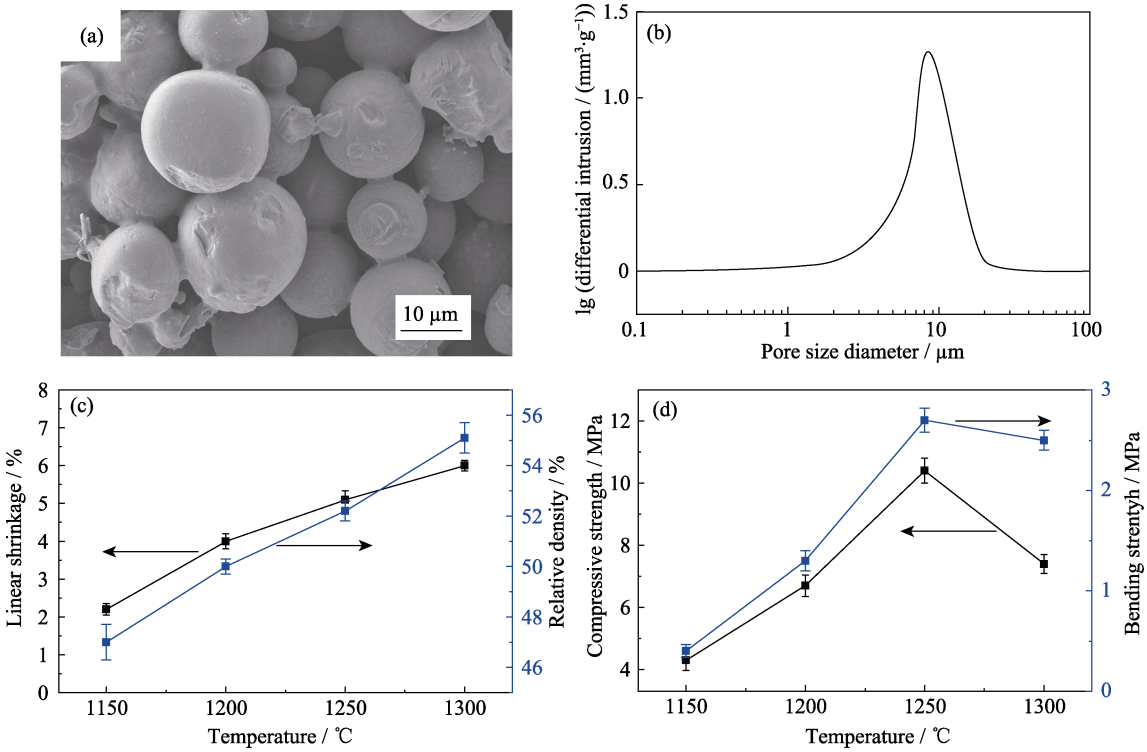

Fig. 7　Characterization of synthesized porous ceramics

(a) SEM image of typical fracture surface; (b) Pore size distribution; (c) Linear shrinkage and relative density; (d) Compressive and bending strength as functions of temperature

The density and linear shrinkage of ceramics increase with the sintering temperature (Fig.7(c)), which is coincident with the basic rule. It is worth noting that the corresponding shrinkage of ceramics is only 5% (1250 ℃) while the ceramics are well sintered, which illustrates the composite spheres are relative stable during the sintering and thus have an advantage in improving the precision of 3D technology.

The mechanical properties of sintered ceramics are also studied, and the results are shown in (Fig. 7(d)). When the temperature increases from 1150 ℃ to 1250 ℃, the compressive and bending strength of ceramics increase to 10.2 and 2.7 MPa, respectively. However, the strength decreases significantly when the sintering temperature reaches 1300 ℃. This is related to the bulk crystallization of β-cristobalite at 1300 ℃, which undergoes β phase to α phase transformation with a volume contraction of about 5vol% when it cools down to 270 ℃, and micro-cracks form in the ceramics[18]. Hence, 1250 ℃ is the most effective temperature for the sintering of composite spheres in 3D production.

3　Conclusions

Spherical SiO_2 particles were firstly employed to synthesize ceramic/resin composite spheres with well dispersity, fine fluidity (25 (s/50 g)) and larger packing density (45.0%) through a simple method. The viscosity of coating media decreased gradually with the temperature increasing or the resin content decreasing, and the most suitable resin content was 27wt%. The spherical shape of ceramic powders was analyzed to be the vital factor for the achievement of uniform coating layers, owing to the interconnected packed pores and the uniform cohesive energy of spheres. The thickness (1.1–3.7 μm) of coating layer could be controlled precisely through changing the pressure during filtration process. The synthesized powders showed well consolidation performance because of the formation of favorite necks among spheres. The ceramic with compressive strength of 10.2 MPa and bending strengths of 2.7 MPa was obtained while the shrinkage was only 5%, which indicated the composite spheres had good prospect in 3D technology.

References

[1] TIWARI S K, PANDE S. Material properties and selection for selective laser sintering process. *Int. J. Adv. Manuf. Tech*., 2013, **27(4/5/6):** 198–217.

[2] LI X M, CAO M J, JIANG Y. Microstructure and mechanical properties of porous alumina ceramic prepared by a combination of 3-D printing and sintering. *Ceram. Int*., 2016, **42(10):** 12531–12535.

[3] MAZZOLI A. Selective laser sintering in biomedical engineering. *Med. Biol. Eng. Comput*., 2013, **51(3):** 245–256.

[4] LYKOV P A, SAPOZHNIKOV S B, SHULEV I S, *et al.* Composite micropowders for selective laser sintering. *Metallurgist*, 2016,

59(9/10): 851–855.

[5] SHAHZAD K, DECKERS J, KRUTH J P, *et al.* Additive manufacturing of alumina parts by indirect selective laser sintering and post processing. *J. Mater. Process. Tech.*, 2013, **213(9):** 1484–1494.

[6] SLOCOMBE A, TAUFIK A, LI L. Diode laser ablation machining of 316L stainless steel powder/polymer composite material: effect of powder geometry. *Appl. Surf. Sci.*, 2000, **168(1–4):** 17–20.

[7] LORRISON J C, DALGARNO K W, WOOD D J. Processing of an apatite-mullite glass-ceramic and an hydroxyapatite/phosphate glass composite by selective laser sintering. *J. Mater. Sci-Mater. M.*, 2005, **16(8):** 775–781.

[8] WANG W, MA S, FUH J H, *et al.* Processing and characterization of laser-sintered $Al_2O_3/ZrO_2/SiO_2$. *Int. J. Adv. Manuf. Tech*., 2013, **68(9/12):** 2565–2569.

[9] DENG Z Y , YANG J F , BEPPU Y, *et al.* Effect of agglomeration on mechanical properties of porous zirconia fabricated by partial sintering. *J. Am. Ceram. Soc*., 2002, **85:** 1961–1965.

[10] SUN Z Q, LI B Q, HU P, *et al*. Alumina ceramics with uniform grains prepared from Al_2O_3 nanospheres. *J. Alloy Compd.*, 2016, **688:** 933–938.

[11] LI B Q, SUN Z Q, HOU G L, *et al.* The sintering behavior of quasispherical tungsten nanopowders. *Int. J. Refract. Met. Hard Mater*., 2016, **56:** 44–50.

[12] YANG S, GWAK J N, LIM T S, *et al.* Preparation of spherical titanium powders from polygonal titanium hydride powders by radio frequency plasma treatment. *Mater. Trans.*, 2013, **54(12):** 2313–2316.

[13] YAN M F, CANNON JR R M, BOWEN H K, *et al.* Effect of grain size distribution on sintered density. *Mater. Sci. Eng*., 1983, **60(3):** 275–281.

[14] LU H M, WEN Z, JIANG Q, *et al.* Nucleus-liquid interfacial energy of elements. *Colloid. Surface A*, 2006, **278(1):** 160-165.

[15] ZHAO J, LU L, ZHANG Z, *et al*. Continuum modeling of the cohesive energy for the interfaces between films, spheres, coats and substrates. *Comp. Mater. Sci*., 2015, **96:** 432–438.

[16] OZER I O, SUVACI E, KARADEMIR B, *et al*. Anisotropic sintering shrinkage in alumina ceramics containing oriented platelets. *J. Am. Ceram. Soc*., 2006, **89(6):** 1972–1976.

[17] JAGOTA A, DAWSON P R. Simulation of the viscous sintering of two particles. *J. Am. Ceram. Soc*., 2010, **73(1):** 173–177.

[18] WILSON P J, BLACKBURN S, GREENWOOD R W, *et al.* The role of zircon particle size distribution, surface area and contamination on the properties of silica-zircon ceramic materials. *J. Eur. Ceram. Soc*., 2011, **31:** 1849–1855.

树脂包覆球形 SiO_2 颗粒制备 3D 打印用陶瓷/树脂复合粉体

孙志强, 杨小波, 王华栋, 李德里, 李淑琴, 吕 毅

(航天特种材料及工艺技术研究所, 北京 100074)

摘 要: 采用球形致密的 SiO_2 微米颗粒制备用于 3D 打印的陶瓷/树脂复合粉体, 并对粉体的固化和烧结性能进行了研究。结果显示, 随着温度升高或固体含量的增加, 包覆介质的粘度逐渐增大, 最佳树脂浓度为 27wt%。均匀包覆的陶瓷/树脂复合粉体具有良好的分散性、流动性(25 (s/50 g))和较大的堆积密度(45.0%)。球形颗粒堆积形成的贯通孔道和球形颗粒表面均匀的吸附能对均匀包覆过程起到了至关重要的作用。包覆层的厚度(1.1~3.7 μm)可以通过调节抽滤过程的负压进行精确控制。由于颗粒之间形成了树脂颈部, 使制备的粉体具有很好的固化强度, 固化的陶瓷生胚经 1250 ℃烧结后获得了性能优异的陶瓷: 压缩强度为 10.2 MPa, 弯曲强度为 2.7 MPa, 烧结收缩仅 5%。上述结果表明, 复合粉体在 3D 打印产业上具有良好的应用前景。

关 键 词: 粉体技术; SiO_2 球; 3D 打印; 包覆层

中图分类号: TB332 **文献标识码:** A